Applications of the Boundary Element Method in Electrochemistry: Scanning Electrochemical Microscopy

Q. Fulian and A. C. Fisher*

Department of Chemistry, University of Bath, Claverton Down, Bath BA2 7AY, U.K.

G. Denuault

Department of Chemistry, University of Southampton, Highfield, Southampton, SO17 1BJ, U.K.

Received: September 16, 1998; In Final Form: December 23, 1998

The boundary element method (BEM) is applied to map the current response of the scanning electrochemical microscope for a range of tip and substrate geometries. Simulations are presented that quantify the diffusional fields around tip electrodes of disk, hemispherical, and cone geometries. Two-dimensional (axisymmetric) simulations examine the effect of the current flowing at the tip electrode as it is brought toward conducting and nonconducting surfaces that are either infinitely flat or spherically distorted. Three-dimensional BEM simulations probe the current response for approach curves where the tip microdisk electrode is not parallel to the substrate surface. The BEM was also applied to simulate a line scan using a microdisk electrode as it is positioned at various points across the surface of a substrate containing a flat macroelectrode. Finally, the three-dimensional routines were employed to produce an image of a single microdisk electrode operating in positive feedback mode embedded in a flat nonconducting substrate. Unlike previous simulations in the research area of scanning electrochemical microscopy the reduction in dimensionality derived by application of the BEM results in a considerable simplification of the grid generation procedures and a substantial reduction in simulation time required. In addition the flexibility of the BEM enables unusual substrate geometries to be addressed that would present considerable difficulties to standard finite difference procedures.

Introduction

Scanning electrochemical microscopy (SECM) has rapidly developed into a powerful tool for the investigation of chemical and electrochemical reactivity.[1−7] To interpret the current response from SECM measurements in terms of physical processes, it has been necessary to develop numerical simulations that quantify the competition between processes such as mass transport and chemical reaction. The majority of workers have adopted a variety of procedures based on the finite difference method (FDM), in much the same way that electrochemical groups have exploited this approach previously.[8−11] However, owing to the point approximation employed, the FDM is not readily adapted to the simulation of electrodes or substrates, which have regions of complex or rapidly changing geometry.

In related fields such as engineering where problems of complex geometry are involved, techniques such as the finite element method (FEM) or boundary element method (BEM) are exploited.[12−16] In the field of SECM where such geometrical complexities are apparent there has been little exploitation of these methods despite their clear potential. Bard[1] previously reported the use of an FEM routine to examine SECM approach curves for a microdisk electrode; however, this has not been exploited further.

In the more general electrochemical field the FEM and BEM have also been substantially overlooked by most workers in comparison to the FDM. Recently, we have employed the FEM to simulate a range of fluid dynamic and diffusion-related problems in electrochemistry[17−21] and demonstrated the benefits of such an approach. In addition we have also recently developed the BEM to simulate diffusion-driven reactions in regions of complex geometry.[22] In this article we exploit the considerable flexibility of the BEM to examine a variety of axisymmetric two-dimensional and three-dimensional diffusion-controlled electrochemical processes occurring at an SECM under various working conditions.

First, we use two-dimensional axisymmetric procedures to simulate approach curves for tip electrodes of microdisk, microhemispherical, sphere-capped, and cone geometries as they approach flat substrates. Next we turn our attention to the influence of substrate shape on the approach curve and illustrate the power and versatility of the BEM to address nonidealized geometries. An insulating, conducting, or mixed insulator/conducting substrate is sequentially distorted from a flat to hemispherical and sphere-capped type geometries of various radii. The shape of the substrate is observed to considerably influence the approach curve response. We also present three-dimensional BEM simulations to examine more complex problems using SECM. Results are presented for approach curves where the tip and substrate are not exactly parallel, a problem that can be encountered in experimental studies. We also present line scans for a microdisk electrode as it sequentially moved across a flat surface containing a macroelectrode. Finally, we illustrate the power of the BEM by producing a full SECM image of a microdisk electrode embedded in an infinitely flat nonconducting substrate operating in positive feedback mode.

The BEM is found to be a powerful and numerically efficient alternative to FDM for the simulation of SECM processes.

Theory

We have previously presented[22] the background information required for the BEM formulation of steady-state one-, two-,

10.1021/jp983732a CCC: $18.00
Published on Web 05/06/1999

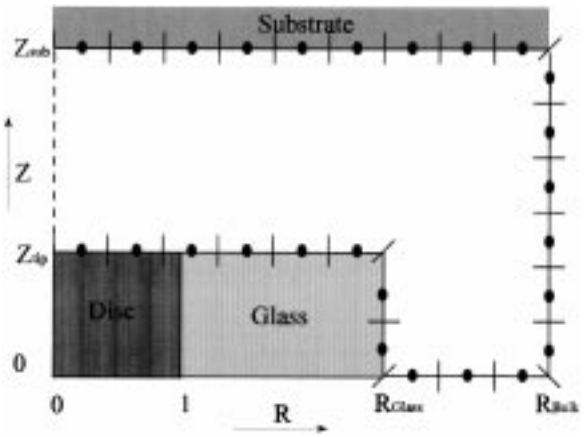

Figure 1. Schematic of the BEM grid and geometry employed for microdisk approach curve simulations.

and three-dimensional solutions of the diffusion eq 1 pertinent to electrolysis under conditions of high supporting electrolyte concentration.

$$D\left(\frac{\partial^2 c}{\partial x^2}\right) + D\left(\frac{\partial^2 c}{\partial y^2}\right) + D\left(\frac{\partial^2 c}{\partial z^2}\right) = 0 \qquad (1)$$

We therefore restrict our discussion here to a brief outline of our general approach and highlighting any differences in our procedures from that reported previously. For the purposes of this paper we shall consider the current response for the reversible one electron-transfer reaction

$$A + e^- \rightleftharpoons B \qquad (2)$$

It is assumed in all the data presented that the SECM tip electrode induces the transport-limited reduction of A at the electrode surface. In the case of the substrate when operating in positive feedback mode[5] the reverse of the SECM tip reaction is induced. In all cases presented the normalization procedures adopted are identical to those employed by Kwak and Bard.[1] Consequently, all distances are normalized with respect to the microelectrode characteristic dimension and concentrations by their bulk value c,[b] consistent with usual practice.[1] The variable d/a is employed to represent the normalized tip−substrate ($Z_{tip} - Z_{sub}$) separation as depicted in Figure 1.

The essential approach of the BEM allows expressions such as eq 1 to be reduced to a boundary-only problem by selection and integration of appropriate weighting functions (G). For the three-dimensional form of eq 1 the integration procedure is performed over x, y, and z coordinates and the fundamental solution satisfies

$$\frac{\partial^2 G}{\partial x^2} + \frac{\partial^2 G}{\partial y^2} + \frac{\partial^2 G}{\partial z^2} = -\delta(x - \xi_1)(y - \xi_2)(z - \xi_3) \qquad (3)$$

where ξ_1, ξ_2, and ξ_3 represent the coordinates of a concentration source. The weighting function is selected as

$$G(x,y,z,\xi_1,\xi_2,\xi_3) = \frac{1}{4\pi r} \qquad (4)$$

where r is the distance between the integration point and the source point

$$r = ((x - \xi_1)^2 + (y - \xi_2)^2 + (z - \xi_3)^2)^{1/2} \qquad (5)$$

Numerical solution proceeds by mapping the boundary of the domain into a series of (boundary) elements. As previously, we have employed triangular elements[22] for these simulations, which take a single fixed flux or concentration over each individual element. The approach requires either the flux or concentration to be defined at each individual element. Solution of the problem then proceeds by generation of a series of simultaneous equations that contain the unknown concentrations or fluxes, thus a fully populated matrix of size ($N_e \times N_e$), where N_e is the number of elements, is created. All routines were written in Fortran 77 or 90 and run on a Pentium 166 PC, with 48 MB Ram. Run times varied between 1 and 20 min for a

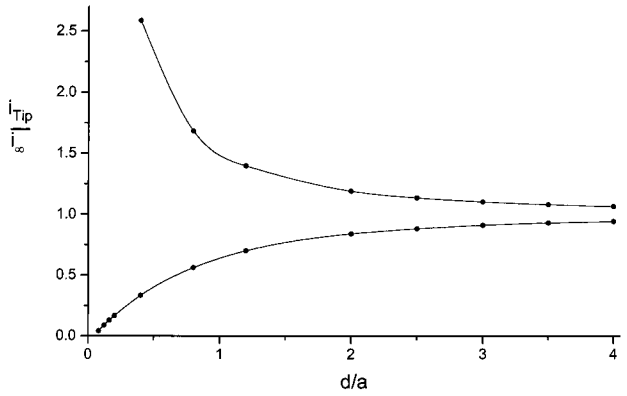

Figure 2. Dimensionless approach curves for hindered and positive feedback modes for a microdisk electrode approaching a flat substrate. Also shown on the plot are the values (●) presented previously in ref 23.

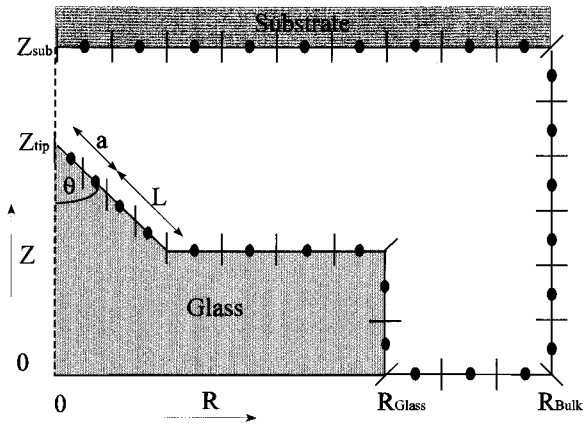

Figure 3. Schematic of the BEM grid and geometry employed for microcone tip approach curve simulations.

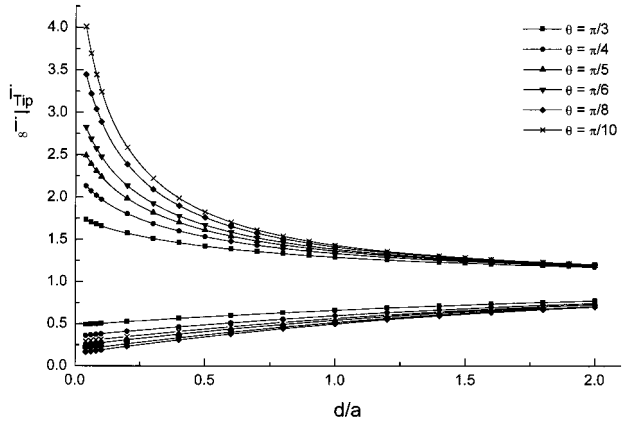

Figure 4. Dimensionless approach curves for hindered and positive feedback modes for a microcone electrode ($a = 1$, $L = 0$) of varying geometry approaching a flat substrate.

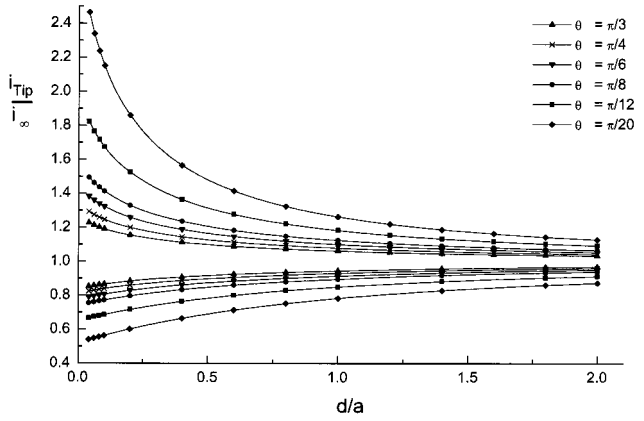

Figure 5. Dimensionless approach curves for hindered and positive feedback modes for a microcone electrode ($a = 1$, $L = 29$) of varying geometry approaching a flat substrate.

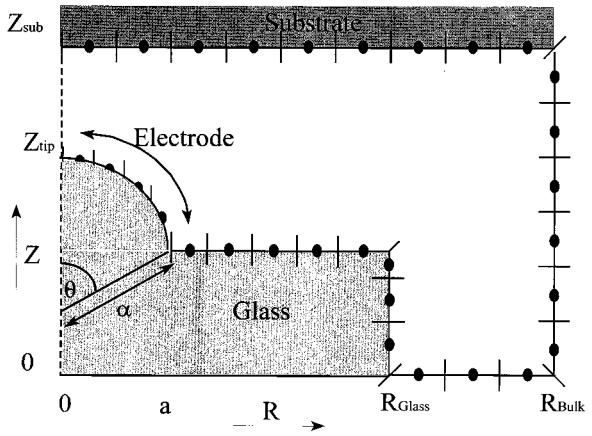

Figure 6. Schematic of the BEM grid employed for microhemispherical tip approach curve simulations.

single steady-state current measurement depending upon the problem of interest.

Results and Discussion

Two-Dimensional Simulations. Initial simulations focused on the application of the two-dimensional axisymmetric codes to examine the current response as a microdisk of radius $a = 1$ embedded within a flat insulating surface of radius ($R_{glass} = 10$) was stepped toward an infinitely flat conducting or nonconducting substrate. The domain of interest was divided into 30 boundary elements (Figure 1), and the following boundary conditions were applied. Typical run times for this

region		insulating substrate	conducting substrate
$1 \geq r \geq 0$	$z = Z_{tip}$	$[A] = 0$	$[A] = 0$
$r = R_{bulk}$	$Z_{tip} > z > Z_{sub}$	$[A] = 1$	$[A] = 1$
$R_{bulk} \geq r \geq 1$	$z = Z_{sub}$	$\partial[A]/\partial Z = 0$	$[A] = 1$
$R_{bulk} \geq r \geq 1$	$z = Z_{tip}$	$\partial[A]/\partial Z = 0$	$\partial[A]/\partial Z = 0$
$r = 0$	$Z_{tip} > z > Z_{sub}$	$\partial[A]/\partial R = 0$	$\partial[A]/\partial R = 0$

case were 60−70 s, and Figure 2 shows the normalized current response for the case where the electrode reaction 2 is induced at the microdisk electrode and the substrate is an insulator. This corresponds to the hindered diffusion mode discussed previously by Bard.[1] Figure 2 also shows the corresponding plot for the case where the substrate is set to reverse reaction 2 and thus is operating in positive feedback mode.[1] Both cases have been reported previously,[23] where it was noted that the value of R_{glass} significantly influences the curve response. Figure 2 also shows

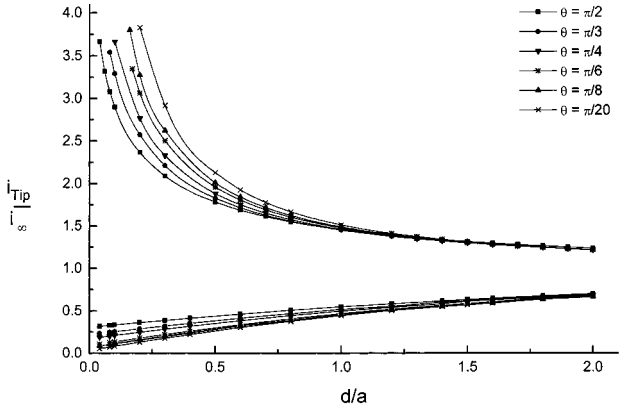

Figure 7. Dimensionless approach curves for hindered and positive feedback modes for microhemispherical electrodes of varying geometry approaching a flat substrate.

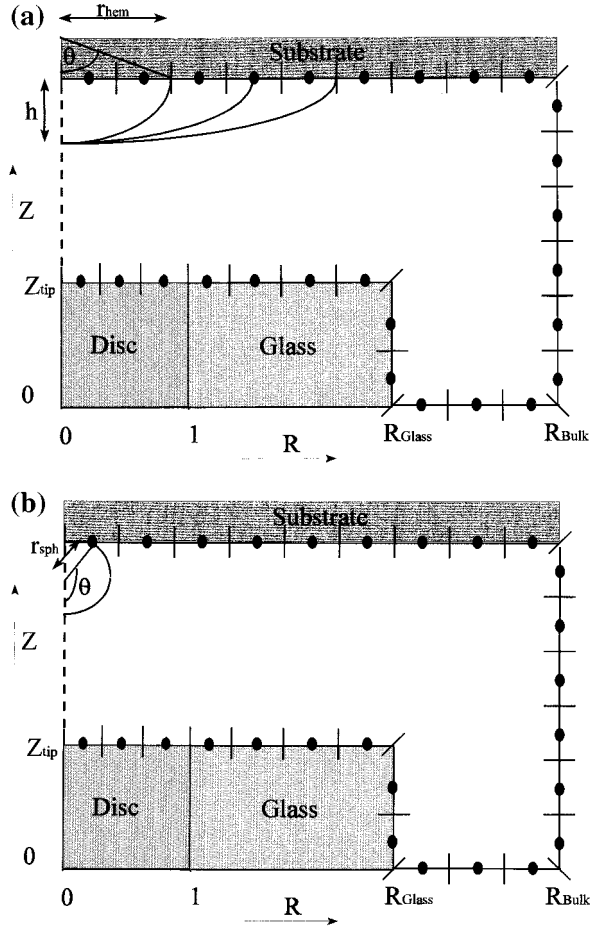

Figure 8. (a) Schematic of the BEM grid employed for approach curve simulations using substrates of varying hemispherical geometry. (b) Schematic of the BEM grid employed for approach curve simulations using substrates of varying sphere−cap geometry.

the results for the correponding case taken from ref 23. Excellent agreement was noted between the two methods. It is apparent that the BEM provides an accurate and highly efficient alternative to the previous methods.

To further explore the flexibility of the BEM, we next examined the case of a cone tip electrode of varying length ($a + L$) approaching an infinitely flat substrate.[24] Figure 3 shows a schematic of the grids employed for this case. The normalized electrode length a was fixed at 1 with the cone length L and angle θ varied to examine the influence on the approach curves for hindered and positive feedback modes. Figure 4 shows the

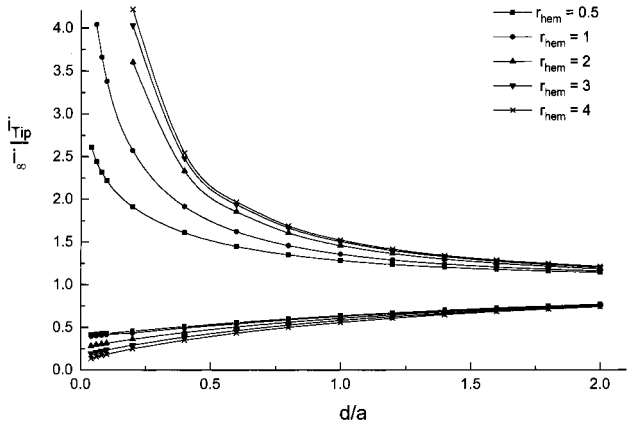

Figure 9. Dimensionless approach curves for hindered and positive feedback modes for a microdisk electrode approaching a microhemispherically distorted substrate of varying radius.

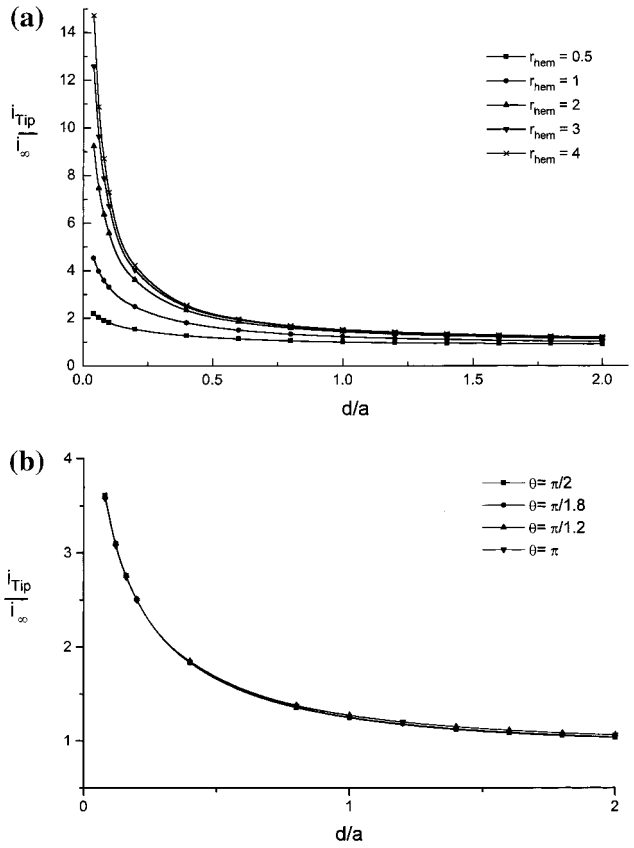

Figure 10. (a) Dimensionless approach curve for a microdisk electrode approaching a mixed insulator/conductor substrate. The microhemispherically distorted region was set in positive feedback mode, and the remainder of the flat substrate set as an insulator. (b) Dimensionless approach curve for a microdisk electrode approaching a mixed insulator/conductor substrate. The sphere−cap distorted region was set in positive feedback mode and the remainder of the flat substrate set as an insulator.

approach curves for the hindered and positive feedback modes where $a = 1$ and $L = 0$, which corresponds to the case where the whole cone is electroactive. Each curve has been normalized with respect to the current response in bulk solution for the specific electrode geometry, and the separation d is defined as the distance from the cone tip to the substrate surface. Next the procedures were repeated for the case $a = 1$ and $L = 29$, which effectively represents a cone of infinite length with a small microcone electrode on the site of the tip. Figure 5 shows the corresponding result for this case using the same normalization prcedures as above.

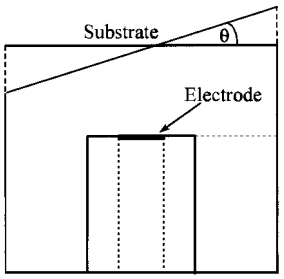

Figure 11. Schematic of the geometry employed for microdisk approach curve simulations with varying tip/substrate angles.

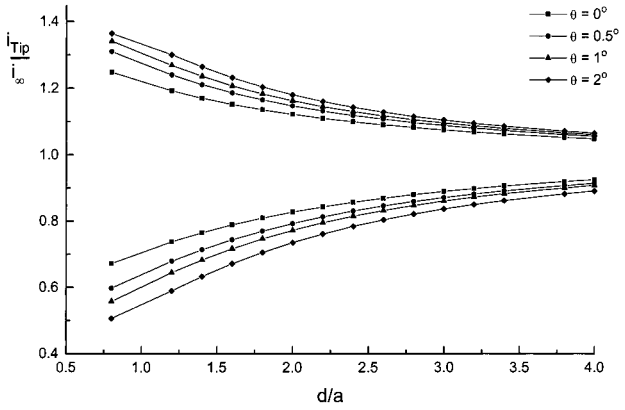

Figure 12. Dimensionless approach curve for a microdisk electrode approaching a flat insulator at various substrate/tip angles.

Next the tip was altered to create a hemispherical type microelectrode (Figure 6) using the following expression to create the electrode surface

$$Z = \frac{a}{\sin\theta} - \frac{a}{\tan\theta}$$

where θ and a are defined in Figure 6. A value of $a = 1$ was employed for each simulation and the value of θ varied to generate various hemispherical/spheroid type electrodes. Approach curves were calculated for hindered and positive feedback modes using a range of values of θ. The distance d was defined from the tip of the hemisphere to the substrate surface. The results are presented in Figure 7.

To further illustrate the versatility of the BEM approach, the influence of substrate shape on the approach curve was examined for a microdisk electrode. Here, the substrate is distorted in a hemispherical manner varying the parameters h and r_{hem} (Figure 8a) and using the expression

$$\frac{R^2}{r_{hem}^2} + \frac{Z^2}{h^2} = 1$$

Figure 9 shows the approach curves for hindered and positive feedback modes where $h = 1$ and r_{hem} was varied between 0.5 and 4. It is apparent that the geometry of the substrate surface strongly affects the approach curve shape. This may be rationalized, since the current density across the surface of the tip microelectrode changes significantly toward the center of the substrate distortion. Next the procedure was repeated for the case of a mixed boundary condition problem. Now the distorted region of the substrate is made to operate in positive feedback mode and the remainder of the substrate is left insulating; the result is shown in Figure 10a.

The approach was repeated for a sphere−cap type geometry, a schematic of which is shown in Figure 8b. The electrode

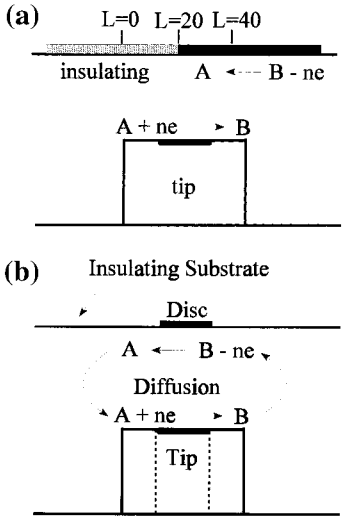

Figure 13. (a) Schematic of the geometry employed for a line scan of a microdisk electrode across a mixed insulator/conductor substrate. (b) Schematic of the geometry employed to produce an SECM image using a microdisk tip and microdisk embedded in a flat substrate.

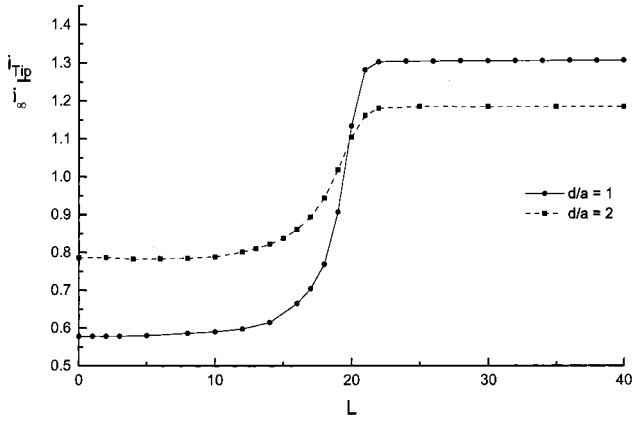

Figure 14. Line scan recorded at two disk−substrate separations over the geometry depicted in Figure 13a.

surface was generated using different values of θ with $r_{sph} = 1$. An approach curve recorded for the case where the sphere−cap geometry operates in positive feedback mode is shown in Figure 10b for varying values of θ.

From above it is apparent that the BEM can be applied to simulate a simple geometric substrate and microelectrode geometries. Extension of these procedures to examine more complex shapes encountered experimentally would only require appropriate grid generation routines. Given the relatively low numbers of elements necessary, it would be feasible to manually define grid data for geometries that do not follow well-defined mathematical forms. The BEM is therefore a powerful tool for the investigation of two-dimensional axisymmetric diffusion problems in SECM.

Three-Dimensional Simulations. Next work focused on application of the three-dimensional diffusion procedures to model the effect of the tip approach angle, the simulation of a single line scan over a substrate surface at different ratios of d/a, and finally an image of a microdisk electrode operating in positive feedback mode.

First we present approach curves for a microdisk electrode embedded in a nonconducting sheath of 10 times the electrode radius as it is brought toward a nonconducting infinitely flat substrate at differing angles to the tip. This problem is typically encountered in experimental investigations, but we are unaware of any previous reports that quantity the influence of this effect. Figure 11 presents a schematic of the problem along with appropriate parameter definitions. The angle θ was varied between 0 and 2° and approach curves recorded for hindered and positive feedback modes of operation. Figure 12 shows the approach curves obtained for the different values of θ, and a significant effect is observed for both modes of operation and results from the variation in height between the tip and substrate.

Next we present results for the movement of a microdisk electrode across the surface of a substrate at two different ratios of d/a. Figure 13a shows a schematic of the problem addressed, the substrate is divided into two regions one-half nonconducting and one-half an electrode set to operate in positive feedback

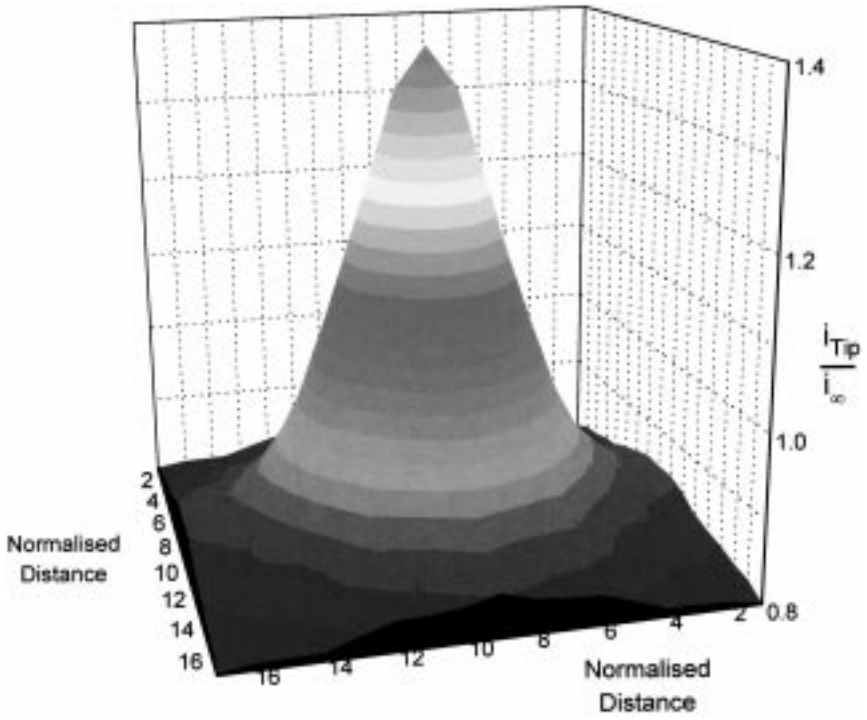

Figure 15. SECM image of the geometry shown in Figure 13b.

mode. Essentially with the appropriate boundary conditions applied this is equivalent to the edge of a macroelectrode embedded in a nonconducting surround. The boundary conditions for this case are similar to the above with the substrate containing a mixed condition that corresponds to no flux over the insulating region and fixed concentration over the region of positive feedback. Figure 14 shows the results for two different tip−substrate separations ($d/a = 2$ and $d/a = 1$) using a microdisk electrode of normalized radius 1 and $R_{glass} = 10$.

It is apparent that the contrast (current magnitude) is strongly dependent on the tip−substrate height, as might be anticipated. It is interesting to note that the resolution does not alter markedly for the two heights. The transition region occurs approximately between $L = 14$ and $L = 22$, where L represents the normalized distance. It is anticipated that higher values of separation would lead to a more drawn out transition in the current response as a function of L.

As a final illustration of the BEM, the three-dimensional codes were used to obtain an image of a microdisk electrode embedded within a nonconducting substrate. This aspect has not been examined previously using numerical techniques owing to the complexity and time requirements for such work. A schematic of the problem addressed is shown in Figure 13b; the electrodes were set to operate in positive feedback mode with the boundary conditions applied in a manner analogous to that above. Figure 15 shows the response for the case where both electrodes have a normalized radius of $a = 1$ and a tip−substrate separation (d/a) of 1. The image was constructed by recording 100 separate steady-state current measurements at regular intervals across the surface, with the substrate electrode positioned at $x = 8$, $y = 8$. The clearly symmetrical shape of the diffusion layer around the electrode is apparent from the image.

In later articles we propose to examine more complex features on substrate surfaces using a range of probe shapes to ascertain the optimal method in terms of resolution.

We have shown that the BEM method can be employed to routinely map a wide range of SECM probe shapes and substrate geometries. The benefits of using the BEM in terms of simulation time and grid generation have been demonstrated, and the approach can be seen to offer an extremely desirable alternative to the traditional methods employed to quantify SECM behavior. Moreover, the extension of the BEM to the simulation of real experimental electrode and substrate configurations is a genuine possibility without more than simple modifications to the grid generation routines. We are currently exploring the possibility of using the BEM to aid in the simulation of potential and concentration distributions for techniques such as STM and AFM when applied to electrochemical problems.

Conclusion

The BEM has been employed to characterize the current density of a number of experimentally important electrode geometries under diffusional mass transport control. The approach has been demonstrated as a flexible and efficient tool for the examination of the current flow as a function of the geometrical influence of electrodes and surrounding insulating regions. The ease of application to electrodes of arbitary geometry offers the possibility of mapping true experimental electrode shapes via scanning probe techniques and simulating the expected response rather than assuming the systems to be idealized shapes contained within a flat surrounding insulator.

Acknowledgment. We thank the University of Bath for a University Studentship for support of Q.F. and the Nuffield Foundation for research support.

References and Notes

(1) Bard, A. J.; Fan, F. R. F.; Kwak, J.; Lev, O. *Anal. Chem.* **1989**, *61*, 132.

(2) Bard, A. J.; Denuault, G.; Lee, C.; Mandler, D.; Wipf, D. O. *Acc. Chem. Res.* **1990**, *23*, 357.

(3) Bard, A. J.; Fan, F. R. F.; Pierce, D. T.; Unwin, P. R.; Wipf, D. O.; Zhou, F.; *Science* **1991** *68*, 254.

(4) Arca, M.; Bard, A. J.; Horrocks, B. R.; Richards, T. C.; Treichel, D. A. *Analyst* **1994**, *119*, 719.

(5) Bard, A. J.; Fan, F. R. F.; Mirkin, M. V. *Electroanal. Chem.* **1994**, *18*, 243.

(6) Fan, F. R. F.; Bard, A. J. *Science* **1995**, *267*, 871.

(7) Wei, C.; Bard, A. J.; Mirkin, M. V. *J. Phys. Chem.* **1995**, *99*, 16033.

(8) Feldberg, S. W. *Electroanal. Chem.* **1969**, *3*, 45.

(9) Britz, D. *Digital Simulation in Electrochemistry*; Sringer Verlag: Berlin, 1981.

(10) Shoup, D.; Szabo, A. *J. Electroanal. Chem.* **1984**, *160*, 17.

(11) Alden, J. A.; Compton, R. G. *J. Electroanal. Chem.* **1996**, *404*, 27.

(12) Ziekiewicz, O. C. *The Finite Element Method in Engineering Science*, 2nd ed.; McGraw-Hill: New York, 1977.

(13) Baker, A. J. *Finite Element Computational Mechanics*, 1st ed.; McGraw-Hill: New York, 1983.

(14) Ramachandran, P. A. *Comput. Math.* **1990**, *19*, 63.

(15) Choi, Y. S.; Kang, T. *J. Electrochem. Soc.* **1996**, *143*, 480.

(16) Yan, J. F.; Pakalapati, S. N. R.; Nguyen, T. V.; White, R. E. *J. Electrochem. Soc.* **1992**, *139*, 1932.

(17) Stevens, N. P. C.; Fisher, A. C. *J. Phys. Chem. B* **1997**, *101*, 8259.

(18) Stevens, N. P. C.; Fisher, A. C. *Electroanalysis* **1997**, *10*, 16.

(19) Stevens, N. P. C.; Fisher, A. C. *J. Ann. Quim.* **1997**, *93*, 225.

(20) Fulian, Q.; Stevens, N. P. C.; Fisher, A. C. *J. Phys. Chem.* **1998**, *102*, 3779.

(21) Stevens, N. P. C.; Gooch, K. A.; Fulian, Q.; Fisher, A. C. *Anal. Chem.*, manuscript submitted.

(22) Fulian, Q.; Fisher, A. C. *J. Phys. Chem. B*, in press.

(23) Amphlett, J. L.; Denuault, G. *J. Phys. Chem.* **1998**, *102*, 9946.

(24) Davis, J. M.; Fan, F.-R.; Bard, A. J. *J. Electroanal. Chem.* **1987**, *238*, 9.